IL NUOVO CIMENTO **40 C** (2017) 192
DOI 10.1393/ncc/i2017-17192-4

COLLOQUIA: LaThuile 2017

PADME: Searching for dark mediator at the Frascati BTF

V. KOZHUHAROV(1)(2) on behalf of the PADME COLLABORATION(*)

(1) *University of Sofia "St. Kl. Ohridski" - Sofia, Bulgaria*
(2) *Laboratori Nazionali di Frascati, INFN - Frascati (Rome), Italy*

received 16 September 2017

Summary. — Massive photon-like particles are predicted in many extensions of the Standard Model with a hidden sector accounting for dark matter candidates. They have interactions similar to the photon, are vector bosons, and can be produced together with photons. Most of the present experimental constraints on the dark photon (A) rely on the hypothesis of dominant decays to lepton pairs. The PADME experiment aims at searching for the $e^+e^- \to \gamma A$ process in a positron-on-target experiment, assuming a decay of the A into invisible particles of the hidden sector. The positron beam of the DAΦNE Beam-Test Facility (BTF), produced by the LINAC at the Laboratori Nazionali di Frascati of INFN, will be used. The core of the experimental apparatus is a fine-grained, high-resolution calorimeter. It will measure with high precision the momentum of the photon in events with no other activity in the detector, thus allowing to measure the A mass as the missing mass in the final state. In about one year data taking, a sensitivity on the interaction strength (ϵ^2 parameter) down to 10^{-6} is achievable, in the mass region from 1 MeV $< M_A <$ 23.7 MeV, running with 6000 positrons in 40 ns long bunches at 550 MeV beam energy. The experiment, now in the construction phase, is planned to run in 2018. The status of the PADME detector and the physics potential of PADME is reviewed.

(*) G. Chiodini, P. Creti, F. Oliva (INFN Lecce); A. P. Caricato, M. Martino, G. Maruccio, A. Monteduro, V. Scherini, S. Spagnolo (INFN Lecce and Dip. di Matematica e Fisica, Università del Salento); P. Albicocco, R. Bedogni, B. Buonomo, F. Bossi, R. De Sangro, G. Finocchiaro, L. G. Foggetta, A. Ghigo, P. Gianotti, M. Palutan, G. Piperno, I. Sarra, B. Sciascia, T. Spadaro, E. Spiriti (INFN Laboratori Nazionali di Frascati); L. Tsankov, (University of Sofia "St. Kl. Ohridski"); G. Georgiev, V. Kozhuharov (University of Sofia "St. Kl. Ohridski" and INFN Laboratori Nazionali di Frascati); F. Ameli, F. Ferrarotto, E. Leonardi, P. Valente (INFN Roma 1); S. Fiore (INFN Roma 1 e ENEA); G. C.Organtini, M.Raggi (INFN Roma 1 e Dip. di Fisica, "Sapienza" Università di Roma); C. Taruggi (INFN Laboratori Nazionali di Frascati e Dip. di Fisica, Università di Roma "Tor Vergata").

1. – Introduction

Despite the great success of the Standard Model (SM) incorporating a huge amount of observed phenomena it still cannot be considered the ultimate theory of the microworld since it fails to explain the lack of antimatter and the nature of the Dark Matter (DM) in the Universe. The solution to these observational facts lies beyond the SM and probing its different extensions is one of the most active direction in the present particle physics.

Few experimental signatures could be used as a guidance for the possible New Physics model —the antimatter excess in the cosmic rays observed by PAMELA [1], *Fermi* [2], and AMS [3, 4]; the unexplained result of the DAMA/LIBRA [5]; the observation of an anomalous excess of events in the inner pair conversion de-excitation of ^8Be [6]. All they can be addressed in the presence of a so-called "Hidden Sector" —a complete new plethora of elementary particles which have zero charges under the SM gauge interactions. A portal —a particle interacting both with the hidden and the visible sector fermions— may act as a connection between the two sectors. Depending on its type, it is possible to distinguish vector portal, Higgs portal, neutrino portal, and axion portal [7].

2. – Dark photon basics

One of the simplest possible realization of the so-called vector portal [8] that does not introduce new scale in the lagrangian is by employing a vector gauge field, the so-called Dark Photon (DP) A', which interacts weakly with the SM fermions

$$\mathcal{L} \sim g' q_f \bar{\psi}_f \gamma^\mu \psi_f A'_\mu, \tag{1}$$

where g' is the universal coupling constant and q_f are the corresponding fermion charges. The term in eq. (1) could be effectively realized also through kinetic mixing of the massive DP with the ordinary photon. Then the interaction of the SM particles with the dark photon will be described by two parameters, $\epsilon \sim g' q_f$ and the dark photon mass $m_{A'}$. The coupling parameter ϵ could also be flavour dependent [9]. The existence of a vector particle with such characteristics may also contribute to the anomalous magnetic moment of the muon [10] and be the origin of the present discrepancy between the theory and the experiment [11].

The dark sector may contain extra degrees of freedom, χ's with mass m_χ, which couple to A' with a relative strength α_D. Depending on the mass hierarchy in the invisible sector, the phenomenology of the events with the dark photon could be divided into two well distinctive scenarios. If $m_\chi > m_{A'}$ then the dark photon decays to SM particles with a rate proportional to ϵ^2. For $m_{A'} < 2m_\mu$ the only allowed final state is the e^+e^-. On the other side, if χ is light and $m_{A'} > 2m_\chi$ then the dominant decay process will be $A' \to \chi\chi$ since it is not suppressed by the small factor ϵ.

The visibly decaying A' scenario was studied extensively in the latest decade while the invisible A' started to get attention only recently.

3. – PADME at DAΦNE Linac

3˙1. *Measurement strategy.* – A suitable reaction to search for invisible A' is the e^+e^- annihilation where the dark photon is produced in association with an ordinary photon. To increase the yield, a positron beam with defined energy will impinge onto a fixed thin target. The search for the process $e^+e^- \to A'\gamma$ will be performed by measuring the

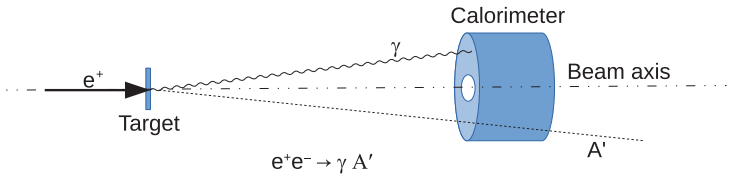

Fig. 1. – A basic idea of the search for dark photon A' with the missing mass technique.

recoil photon position and energy, as shown schematically on fig. 1. The single kinematics quantity, the missing mass, is calculated according to

$$M^2_{miss} = (P_{e+} + P_{e-} + P_\gamma)^2, \tag{2}$$

where P_{e+} is obtained from the known beam momentum, P_{e-} is assumed as $(m_e, 0, 0, 0)$ (electrons in atoms are taken to be at rest, compared to the much higher beam energy) and P_γ is calculated using the measured energy E_γ and the impact point of the accompanying photon in the electromagnetic calorimeter.

The dominant background contributions in the missing mass approach are [12]:

- Radiative emission of photons. This could proceed either through the interaction of the beam positrons in the field of the nuclei (bremsstrahlung) or through a radiative Bhabha scattering on the atomic electrons.
- Two photon annihilation. The missing mass distribution for $e^+e^- \to \gamma\gamma$ events peaks at zero.
- Multiphoton annihilation. The presence of extra photons leads to a missing mass distribution that is not peaked at zero. In addition, some of the photons may escape outside the acceptance of the calorimeter which decreases the rejection power for such events.

The Positron Annihilation into Dark Matter Experiment (PADME) [13,14] is designed to minimize the background contribution while keeping high acceptance for $e^+e^- \to A'\gamma$ events. It is shown schematically in fig. 2 and consists of a target region, a crystal calorimeter, a dipole magnet, a set of charged particle detectors exploiting the magnetic field to detect positrons and electrons, a small angle photon veto, and a specialized detector to facilitate the initial beam tuning and to provide precise measurement of the particle flux in the beam.

The dipole magnet of PADME is MBPS type on loan from CERN, with a total length of 1 m and width of 52 cm. The gap between the poles was extended to 23 cm and a detailed mapping of the magnetic field was performed. The magnet is placed downstream the target and deflects the nominal positron beam outside the calorimeter acceptance. An evacuated chamber, part of the experimental setup, decreases to a negligible level the background from beam-gas interactions. A short description of the PADME major components follows.

3˙2. *PADME at BTF.* – PADME will be located in the existing Beam Test Facility hall [15] at LNF-INFN, as shown in fig. 3. The positron beam is taken from the DAΦNE Linac which major purpose is to provide electrons and positrons with energy of 510 MeV to the DAΦNE storage ring. At nominal operation the Linac is able to deliver a total

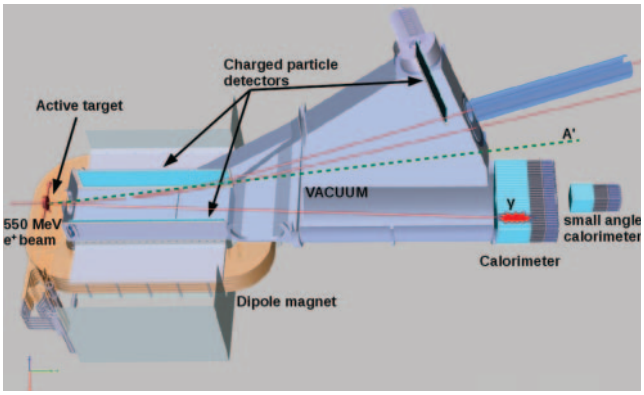

Fig. 2. – Schematics of the PADME experiment setup.

ot 49 bunches per second, each with duration up to 10 ns. For PADME, the accelerator will be operated in a dedicated mode allowing to provide positrons with energy of 550 MeV and a bunch duration of at least 40 ns. The beam energy spread is below 1% and the beam divergence is of the order of 1mrad for a beam spot of the order of 1 mm both in X and Y axis.

The PADME sensitivity to the dark photon parameters depends crucially on the available statistics and the duty cycle of the Linac. Since the bunch rate cannot be increased to more than 49 per second an extensive effort was invested to study the operation and the beam parameters with an increased bunch length. A stable beam with duration of 160 ns was achieved with indications that this could be further increased to more than 200 ns [16]. In addition, to ensure non-interrupted operation of PADME and to preserve the possibility to exploit the beam from the Linac for test purposes, a new BTF hall with a corresponding beam line is currently under construction.

Fig. 3. – Location of the PADME setup toghether with the upgraded beam test facility.

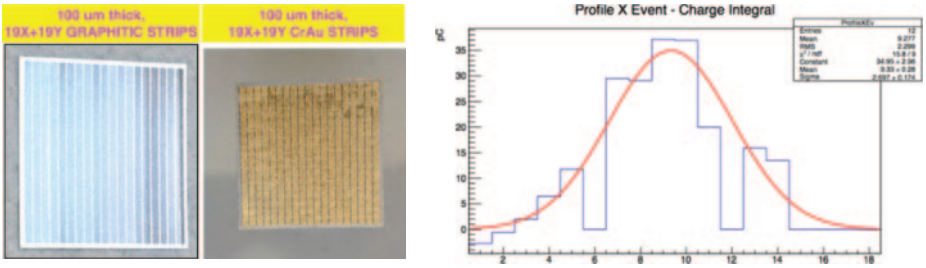

Fig. 4. – Left: a photo of the diamond targets; Right: BTF beam profile as measured by the prototype of the PADME diamond detector, with strip index on the X axis.

3˙3. *Active target*. – The center of the beam spot at the interaction target is used to compute the recoil photon four-momentum in the calculation of the missing mass. Although the individual bunches from the Linac have spot size below 1 mm, their center may vary from bunch to bunch in a long-term operation. To measure the central position of each bunch PADME will employ an active target which will also provide information about the particle multiplicity in the bunch. The target will be made of large area (20 mm $\times$ 20 mm) policrystaline diamond with thickness of 100 μm [17]. Strips in X and Y axis will provide the position measurement.

Different prototypes of the diamond active target, shown in fig. 4 (left), have been tested so far, both with metalizated and with nano-graphitic electric contacts realized with a 193 nm UV ArF excimer laser. The nano-graphitic strips are the preferred choice for PADME since this will result in a fully carbon target. A profile of the beam was obtained during a test at the BTF is shown in fig. 4 (right). The obtained resolution on the position of the beam center was better than 200 μm.

The target front-end electronics will be based on the AMADEUS chip from IDEAS which hosts 16 charge sensitive pre-amplifiers with outputs fed to digitizers.

3˙4. *Calorimeter*. – The calorimeter will serve to measure the energy and the impact point of the recoil photon. To obtain optimal missing mass resolution the calorimeter should provide very good energy (comparable to the beam energy spread) and position resolution (comparable to the beam spot size). The radiative photons yield to extreme occupancy in the central part of the electromagnetic calorimeter. That is why it is made as a ring-shaped structure without any active material close to the beam axis.

The detector will be made of 616 BGO crystals refurbished from the end-cap of the L3 calorimeter. The crystals, annealed to recover their transparency, will be machined to dimensions $21 \times 21 \times 230\,\mathrm{mm}^3$ and will be arranged to form a cylindrical structure with a diameter of $\sim$600 mm and length of 230 mm, as shown in fig. 5 (left). The light will be collected by 19 mm diameter HZC XP1911 photomultipliers.

A prototype with a matrix of 5×5 crystals was constructed and tested at the BTF in 2016, using the facility in single electron mode [18]. The measured energy resolution, shown in fig. 5 (right), is $\sigma(E)/E = 2.0\%/\sqrt{E} \oplus 0.003\%/E \oplus 1.15\%$, where E is in GeV, and is consistent with PADME requirements.

In addition to the BGO calorimeter, an ultra-fast Cerenkov electromagnetic calorimeter will placed along the undeflected beam axis further downstream. Because of the rate of the radiative photons it should provide excellent double pulse separation to be able to veto efficiently multiphoton annihilation events.

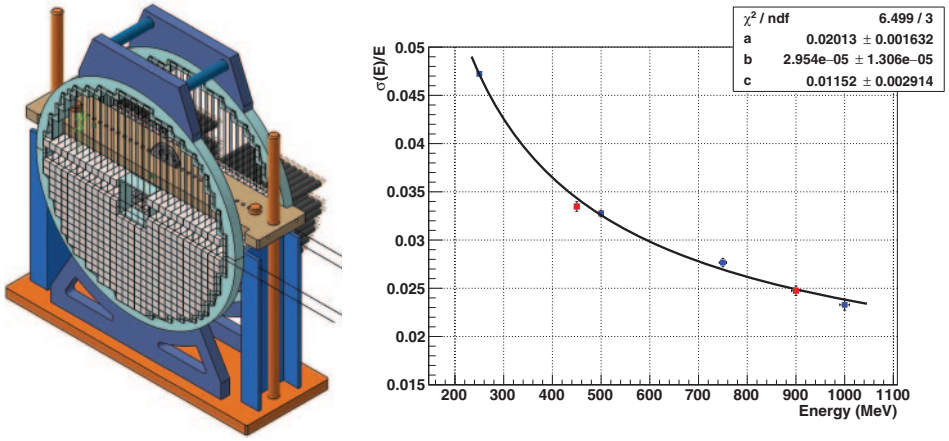

Fig. 5. – Left: design of the PADME calorimeter; Right: measured energy resolution as a function of the deposited energy in the calorimeter prototype [18].

3˙5. *Charged particle detectors*. – The positrons that radiate a photon in the target will have lower momentum and will be stronger deflected by the dipole magnetic field. They will be detected by a charged particle detector composed by an array of polystyrene plastic scintillator bars, each with dimensions $10 \times 10 \times 184\,\mathrm{mm}^3$. A 1.2 mm diameter BCF-92 wave-length shifting (WLS) fiber is placed in a groove along the bar for the collection of the scintillation light. Few prototypes (one of them shown in fig. 6(left)) were constructed and tested at the BTF, showing that detection efficiency higher than 99% and time resolution better than 1 ns is achievable.

The light from the WLS fiber is detected by a $3 \times 3\,\mathrm{mm}^2$ Hamamatsu silicon photomultiplier which is placed on a custom developed PCB, shown in fig. 6 (right). The PCB hosts a transimpedance amplifier and provides the operational voltage, set by an additional controller through an $\mathrm{I}^2\mathrm{C}$ bus. Preliminary tests with the presented detector and electronics indicate a single channel time resolution of the order of 700 ps.

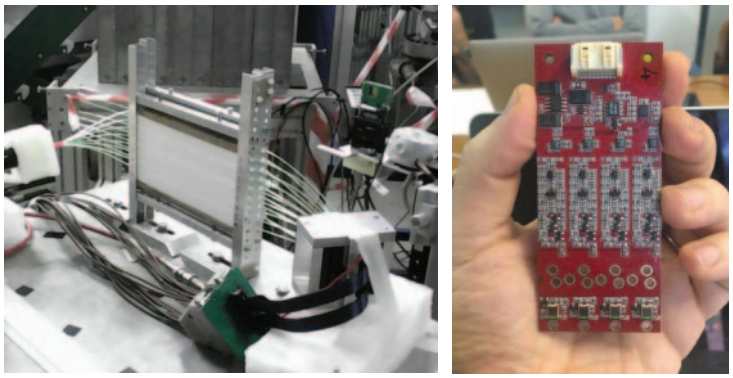

Fig. 6. – Left: a photo of a prototype made of plastic scintillator bars and WLS fibers, placed for test at the BTF; right: a photo of the front-end card with four SiPMs.

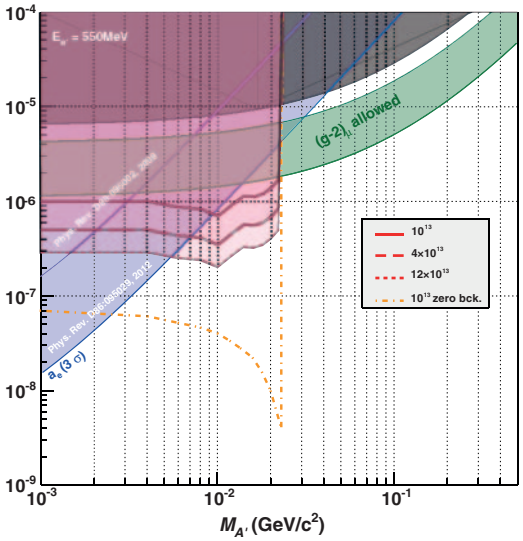

Fig. 7. – Projection of the PADME reach in the ϵ^2 and $m_{A'}$ plane.

A set of three charged particle detectors will be placed in the PADME setup —two inside the magnet on the positron and the electron deflection sides, and another one further downstream to detect positrons with energy loss less than 100 MeV.

4. – Sensitivity and physics case

A full Geant4 based Monte Carlo simulation of the PADME setup [19] was performed to address the background and the acceptance efficiency for the signal events. The cross-section for the $e^+e^- \to A'\gamma$ process for a given value of the parameters ϵ^2 and $m_{A'}$ was calculated using CalcHEP [20].

With 1 ns time resolution of the calorimeter and the charged particle veto detectors the total number of positrons per bunch is limited by the probability for overlapping events and amounts to ∼5000 positrons for a nominal bunch duration of 40 ns. This corresponds to about 10^{13} positrons-on-target per two years, at 50% data taking efficiency.

The projected sensitivity of PADME to the existence of invisibly decaying dark photon in the ϵ^2 and $m_{A'}$ parameter space is given in fig. 7. With 10^{13} positrons-on-target it is possible to reach sensitivity down to $\epsilon^2 \sim 10^{-6}$. Moreover, an increase of the statistics profitting from the ongoing BTF upgrades will improve the results significantly.

PADME is also sensitive to any new light particles, including scalars and pseudoscalars, that are produced in the positron-on-target interactions. An estimation of the physics potential of PADME to search for axion like particles as well as other exotic states is ongoing. In addition, it will be possible to perform measurements of the differential cross sections for bremsstrahlung emission for positrons in the O(100 MeV) energy range and to address the multiphoton annihilation cross sections.

5. – Conclusion

PADME will be the first experiment to search for dark photons in positron-on-target annihilation process. The experiment is currently under construction. The data taking is expected to start in spring 2018 with O(200 ns) bunch duration which will result in the collection of about 10^{13} positrons-on-target by the end of 2018. This will allow to probe the existence of a dark photon in the mass region 1 MeV $< M_A <$ 23.7 MeV for relative coupling strength down to 10^{-6}.

* * *

The author acknowledges support from LNF-INFN under agreement LNF-SU 70-06-497/07.10.2014 and Bulgarian National Science Fund under contract DN-08-14/14.12.2016.

REFERENCES

[1] PAMELA Collaboration (Adriani O. *et al.*), *Nature*, **458** (2009) 607.
[2] Fermi LAT Collaboration (Ackermann M. *et al.*), *Phys. Rev. Lett.*, **108** (2012) 011103.
[3] AMS Collaboration (Aguilar M. *et al.*), *Phys. Rev. Lett.*, **110** (2013) 141102.
[4] AMS Collaboration (Aguilar M. *et al.*), *Phys. Rev. Lett.*, **117** (2016) 091103.
[5] Bernabei R. *et al.*, *Eur. Phys. J. C*, **67** (2010) 39.
[6] Krasznahorkay A. J. *et al.*, *Phys. Rev. Lett.*, **116** (2016) 042501.
[7] Jim Alexander *et al.*, arXiv:1608.08632 [hep-ph].
[8] Holdom B., *Phys. Lett. B*, **166** (1986) 196.
[9] Raggi M. and Kozhuharov V., *Riv. Nuovo Cimento*, **38** no. 10 (2015) 449.
[10] Pospelov M., *Phys. Rev. D*, **80** (2009) 095002.
[11] The g-2 Collaboration(Benett G. W. *et al.*), *Phys. Rev. D*, **73** (2006) 072003.
[12] Kozhuharov V., *EPJ Web of Conferences*, **142** (2017) 01018.
[13] Raggi M. and Kozhuharov V., *Adv. High Energy Phys.*, **2014** (2014) 959802.
[14] Raggi M., Kozhuharov V. and Valente P., *EPJ Web of Conferences*, **96** (2015) 01025.
[15] Ghigo A. *et al.*, *Nucl. Instrum. Methods A*, **515** (2003) 524.
[16] Valente P. *et al.*, arXiv:1603.05651 [physics.acc-ph].
[17] Chiodini G. (PADME group), *JINST*, **12** (2017) C02036.
[18] Raggi M. *et al.*, *Nucl. Instrum. Methods A*, **862** (2017) 31.
[19] Leonardi E. *et al.*, talk and proceedings of CHEP 2016, contribution ID 241 (2016).
[20] Pukhov A. *et al.*, Preprint INP MSU, 98-41/542 (1999) arXiv:hep-ph/9908288; Pukhov A., arXiv:hep-ph/0412191.